

## RESEARCH ARTICLE

# Clinical Scenario and Imaging with Illustrations of Giant Cell Tumor of Bone: A Retrospective Analysis

Nadeem Ali, MS Orthopaedics<sup>1</sup>; Azad Ahmad Shah, MS, DNB Orthopaedics<sup>1</sup>; Ibreez Rakshan, MBBS<sup>1</sup>;

Altaf Ahmad Kawoosa, MS Orthopaedics<sup>1</sup>; Mohammad Umar Mumtaz, MS Orthopaedics<sup>1</sup>

Research performed at Department of orthopaedics, Govt Medical College Srinagar, India.

Received: 02 August 2020

Accepted: 03 April 2021

## Abstract

**Background:** The giant cell tumour of the bone has a spectrum of clinical-radiological presentation. This study aims to describe this varied presentation in our institution.

**Methods:** This retrospective study was conducted on twenty-nine pathologically labelled cases of giant cell tumours of the bone. The medical records for their clinical presentation and diagnostic imaging studies were studied and evaluated.

**Results:** Mean age of the patients at presentation was 35.3±12.9 years. Pain, local swelling and restricted joint function were seen in 93 %, 58.6 % and 52 % patients, respectively. The cortical breach was seen in 15 (51.7 %) and 22 (75.9 %) lesions on plain radiographs and CT images, respectively. 14(48.3 %) cases had soft tissue invasion on MRI at presentation. 26 (89.7 %) lesions were located within 1 cm from the articular cartilage. The solid tumour component was hypo to iso-intense in signal intensity in 27 (93.1 %) lesions in T1 weighted and 21 (72.4 %) in T2 weighted images. 14 (48.3 %) had hyperintense cystic areas, and fluid-fluid levels, suggestive of aneurysmal bone cysts, were seen in 4 (13.8 %) cases on T2 weighted images. Hypo-echoic nodular areas in solid tumour component, suggestive of hemosiderin deposits, were present in 3 (10.3 %) lesions on T1 and T2 weighted images.

**Conclusion:** The tumour classically presents as an epiphysial-metaphyseal, eccentric, expansile, lytic lesion in a skeletally mature patient. The MRI picture is variable and the surgeon should have a sound knowledge of these variations to obtain a biopsy sample from a proper site of the lesion and to avoid misdiagnosis especially of a primary ABC.

**Level of evidence:** IV

**Keywords:** Giant-Cell, Soap-Bubble, Hemosiderin, Fluid-Fluid, ABC

## Introduction

**G**iant cell tumour of bone (GCTB) is a common bone pathology which constitutes around 20 % of the benign bone tumours. (1) It differs from other benign bone neoplasms in its local aggressiveness. Along with chondroblastomas, it is the only benign bone tumour that can have distant metastasis with a reported incidence of 1 to 9 %. (2) Not only does its biological behaviour, which ranges from a latent

benign to a highly recurrent and occasionally of metastatic potential, but also does its radiological picture present high variability. It may present radiologically as a spectrum from a well-defined geographic lesion to a locally aggressive lesion which destroys the bone. (3) In this article, we discuss the clinical presentation and imaging features of the GCTB in a series of patients evaluated at our centre.

**Corresponding Author:** Nadeem Ali, Hospital for Bone and Joint Surgery Barzulla, Associated hospital of Govt Medical College Srinagar, India.

Email: drnadeem@gmail.com



THE ONLINE VERSION OF THIS ARTICLE  
ABJS.MUMS.AC.IR

### Materials and Methods

This retrospective study was conducted on the patients, with a histopathological diagnosis of giant cell tumour of the bone, that attended our institution from 2015 to 2019. The medical records and the imaging studies which included plain radiographs, CT scan, MRI scan of the pathologic bone and chest radiographs of these patients, were evaluated. A total of 36 patients were identified. Seven patients were excluded because of incomplete records or incomplete imaging studies. 29 patients qualified for this study. The demographic and clinical details of the patients which included age, sex, laterality, bone involved, and presenting symptom(s) were recorded. The imaging studies were read by a single senior radiologist and the following radiological parameters were recorded: region(s) of the bone involved by the tumour (epiphyseal, metaphyseal, diaphyseal or a combination of these); relation of long axis of tumor with the long axis of the bone (eccentric or centric); presence of cortical expansion or expansile remodelling; cortical erosion or scalloping; breach in the cortex; Campanacci grade (Grade 1, 2 or 3); nature of the transition zone of the lesion (narrow or wide), type of bone lesion (geographic, permeative or moth eaten); presence of sclerotic rim in geographic lesions (no rim, fine hairline or thick sclerotic rim); presence or absence of pseudo trabeculations (honey comb or soap bubble appearance of the lesion); associated pathological fracture at the tumor site; soft tissue extension of the lesion; change in the contour of the articular surface; invasion of the joint by the tumor; minimum distance between the tumor margin and the articular cartilage ( $\leq 5$ mm, 5 to 10 mm or  $>10$  mm); signal intensity of the tumor (solid component) on T1 weighted and T2 weighted images (hypo, iso or hyperintense); homogenous or heterogeneous signal intensity; presence or absence of cystic components and fluid-fluid levels suggestive of secondary aneurysmal bone cysts (SABC) on T2 weighted images; features of hemosiderin deposition on MRI; and presence of pulmonary metastasis. The collected data were analysed by using SPSS software, version 22.0, for Windows (SPSS, Chicago, IL, USA). Continuous variables were expressed as mean  $\pm$  SD (standard deviation) with its respective range. Nominal and ordinal variables were expressed as proportions.

### Results

The age of the patients ranged from 18 to 65 years with a mean of  $35.3 \pm 12.9$  years. The majority of the patients ( $n = 16, 55.1\%$ ) were in their third and fourth decade of their life.  $79.3\%$  ( $n = 23$ ) patients were in the age group of 21 to 50 years. Females were slightly affected more with a male to female ratio of 1:1.2. The left side was involved more commonly than the right side with a ratio of 1.9:1. The most common site of location was the proximal tibia ( $31\%$ ,  $n=9$ ) followed by the distal femur ( $17.2\%$ ,  $n=5$ ), distal radius ( $10.3\%$ ,  $n=3$ ), pelvis ( $10.3\%$ ,  $n=3$ ), proximal humerus ( $6.9\%$ ,  $n=2$ ), and the distal ulna ( $6.9\%$ ,  $n=2$ ). The distal tibia, proximal femur, distal humerus, proximal

fibula and talus were involved, one patient each ( $3.4\%$ ). Hence, the long bones were involved in  $86.2\%$  ( $n = 25$ ) patients, flat bones in  $10.3\%$  ( $n=3$ ) and the small bones of the hand and feet in only  $3.4\%$  ( $n=1$ ) cases. The pain was the major symptom ( $93\%$ ,  $n=27$ ) followed by the local swelling ( $58.6\%$ ,  $n=17$ ).  $52\%$  ( $n=15$ ) of patients had some degree of restriction of the adjacent joint function (Table 1).

The most common site of the long bones involved was the epiphyseal-metaphyseal ( $44\%$ ,  $n=11$ ) and metaphyseal-epiphyseal ( $44\%$ ,  $n=11$ ) region. Epiphyseal-metaphyseal-diaphyseal involvement was seen in two ( $8\%$ ) patients and pure metaphyseal in only one ( $4\%$ ) patient. In the long bones, most of the lesions ( $64\%$   $n= 16$ ) had an eccentric location and the remaining  $36\%$  ( $n=9$ ) lesions were centric (Figure 1a, 1b). Cortical expansion or expansile remodelling was seen in  $65.5\%$  ( $n = 19$ ) patients while as all had cortical thinning or scalloping (Figure 1c, 1d). On simple radiographs, a breach in the cortex of the bone was demonstrable in  $51.7\%$  ( $n = 15$ ) of the lesions and this number increased to  $75.9\%$  ( $n = 22$ ) on examination of the CT scan images (Figure 1e, 1f).

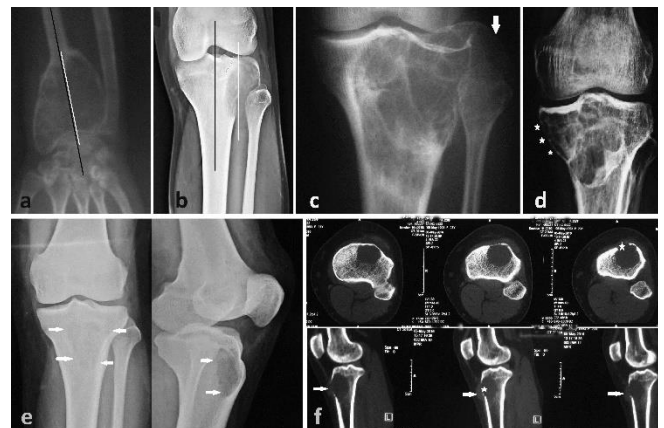


**Figure 1.** (a, b) Relation of tumour axis (white line) with the long axis of the bone (black line). (a) Centric lesion. (b) Eccentric lesion. (c) Expansile remodelling (arrow) of lateral condyle of the tibia. (d) Cortical thinning (stars) of the medial cortex. (e, f) GCT of the proximal tibia. (e) Radiograph showing lytic lesion (arrows) in metaphysis with intact cortices. (f) CT axial and sagittal cut sections showing breach in the anterior cortex (star) with soft tissue extension (arrow).

The Campanacci grading was based purely on the simple radiographs and  $51.7\%$  ( $n = 15$ ) were grade 3 lesions while the remaining  $48.3\%$  ( $n=14$ ) were grade 2 with no grade 1 lesions seen in our series.  $76\%$  ( $n=22$ ) of the lesions had a narrow zone of transition (geographic lesions) on radiographs.  $59\%$  ( $n =13$ ) of the geographic lesions had a poorly appreciable fine hairline like sclerotic rim at the transition zone,  $22.7\%$  ( $n = 5$ ) had well demonstrable sclerotic rim while  $18.2\%$  ( $n = 4$ ) had no such sclerotic rim at the transition (Figure 2a, 2b, 2c).



**Figure 2. (a) Well defined sclerotic rim (white arrows). (b) Hardly visible fine hairline (black arrows) like sclerosis. (c) Well marked demarcation (white arrow) between normal bone and lesion but no sclerotic rim. (d) Permeative lesion with a wide zone of transition (inside the rectangle).**

24 % (n=7) were permeative lesions with a wide zone of transition (Figure 2d). Pseudo-trabeculations were seen on radiographs in part or whole of the lesion in 62.1 % of the cases (n=18) (Figure 3a). Three (10.3 %) cases were complicated by a pathological fracture (Figure 3b; Table 1).



**Figure 3. (a) Expansile lesion with cortical scalloping and pseudo-trabeculation of the lytic lesion (soap bubble appearance). (b) GCT of the proximal tibia with associated pathological fracture.**

**Table1. Radiological features**

Parameter		Frequency
Location in long bones (n = 25)	Epiphyseal-metaphyseal	44 % (n = 11)
	Metaphyseal-epiphyseal	44 % (n = 11)
	Epiphyseal-metaphyseal-diaphyseal	8 % (n = 2)
Centricity in long bones (n = 25)	Metaphyseal	4 % (n = 1)
	Centric	36 % (n=9)
	Eccentric	64 % (n = 16)
Cortical expansion		65.5 % (n = 19)
Cortical breach	On plain radiograph	51.7 % (n = 15)
	On computed tomography	75.9 % (n = 22)
Campanacci Grade	Grade 1	0 % (n = 0)
	Grade 2	51.7 % (n = 15)
	Grade 3	48.3 % (n = 14)
Type of lesion	Geographic	44.8 % (n = 13)
	Hairline sclerotic rim	
	Thick sclerotic rim	17.2 % (n = 5)
	No sclerotic rim	13.8 % (n = 4)
	Moth-eaten / Permeative	24.1 % (n = 7)
Pseudo-trabeculations		62.1 % (n = 18)
Pathological fracture		10.3 % (n = 3)
Soft tissue extension		48.3 % (n = 14)
Joint	Distorted articular cartilage	34.5 % (n = 10)

involvement	Joint infiltration	13.8 % (n = 4)
Relation of tumour margin with subchondral bone	≤ 5mm	89.7 % (n = 26)
	5 -10 mm	13.8 % (n = 4)
	> 10mm	6.9 % (n = 2)
MRI T1 imaging (solid tumor component)	Hypo-intense	62.1 % (n = 18)
	Iso-intense	31.0 % (n = 9)
	Hyper-intense	6.9 % (n = 2)
MRI T2 imaging (solid tumour component)	Hypo-intense	69.0 % (n = 20)
	Iso-intense	3.4 % (n = 1)
	Hyper-intense	27.6 % (n = 8)
Cystic components		48.3 % (n = 14)
Fluid-fluid levels (Secondary ABC)		13.8 % (n = 4)
Hemosiderin deposits		10.3 % (n = 3)

ABC: Aneurysmal Bone Cyst

Some degree of soft-tissue extension was demonstrable on the MRI images in about 48.3 % (n=14) of the lesions (Figure 4a).



**Figure 4. (a) Axial and coronal MRI sections showing soft tissue invasion (black stars) of GCT through a breach in the anterior cortex of the tibia. (b) MR axial cut section of GCT of lateral femoral condyle showing the distorted contour of patella-femoral joint (arrow). (c) GCT proximal tibia with depression (arrow) of part of the lateral tibial articular surface. (d, e) GCT of the distal radius. (d) MRI showing tumour invasion of soft tissue and wrist joint. (e) Clinical picture showing tumour mass at the radial styloid.**

The contour of the articular cartilage was distorted in 34.5 % (n=10) of the cases, with joint infiltration by the tumour seen in 13.8 % (n =4) cases only (Figure 4b, 4c, 4d, 4e). On MRI, the tumour margin was within 5 mm range from the articular cartilage in 89.7 % (n =26), within 5 to 10 mm in 13.8 % (n = 1) and within ≥ 10 mm range in 6.9 % (n =2) of the lesions. Overall, 89.7 % of the lesions were within 1 cm range from the articular cartilage. The signal intensity of the lesion on T1 weighted image was hypo-intense in 62.1 % (n = 18), iso-intense in 31 % (n = 31 %) and hyper-intense in 6.9 % (n = 2) of the cases (Fig. 5a). However, on T2 weighted imaging, 51.7 % (n=15) of the lesions had homogenous intensity while the rest had heterogeneous signal intensity. The solid component of the lesion was hypo-intense in 69 % (n = 20) lesions, hyper-intense in 27.6 % (n = 8) and iso-intense in only one lesion on T2-weighted imaging (Figure 5b). Hyper-intense cystic components were seen in 48.3% (n=14) of the lesions on T2 weighted images (Figure 5c).

Four patients (13.8 %) had demonstrable fluid-fluid levels suggestive of secondary ABCs on T2 weighted images (Figure 6a, 6b). Demonstrable hemosiderin deposits seen as hypoechoic areas with much lower signal intensity than solid tumour component were seen in 3 lesions (10.3 %) (Figure 6c, 6d; Table 1). Metastasis of the tumour to lungs was seen on plain chest radiographs at the presentation in two cases (6.9 %) (Figure 7a, 7b; Table 1).



Figure 5. (a, b) Coronal cut MRI images showing GCT of the lateral tibial condyle. (a) T1 weighted image showing iso-intense signal of the lesion with respect to the muscle. (b) T2 weighted image showing hyper-intense signal of the lesion. (c) Sagittal cut section MRI (T2 image) with a heterogeneous signal with predominant hyper-intense cystic lesions.



Figure 6. (a, b) GCT of the proximal tibia. (a) Iso-intense signal (star) on T1. (b) T2 weighted cross-sectional image showing heterogeneous signal intensity with multiple cysts and fluid-fluid levels (black arrow). (c, d) MR sagittal cut sections of GCT of the proximal tibia. (c) T1 weighted image with hypoechoic nodular lesions (star) suggestive of hemosiderin deposits. (d) T2 weighted image with similar hypoechoic nodular lesions of hemosiderin deposits.

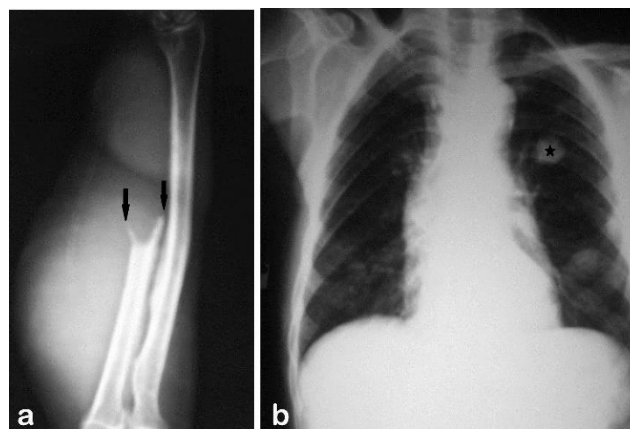


Figure 7. (a, b) GCT of the distal ulna with lung metastasis at presentation. (a) Radiograph showing destruction of the distal half of ulna with diverging cortices (black arrows) suggestive of an expansile lesion. (b) Metastatic lung nodule (black star).

### Discussion

GCTB has been defined as a locally aggressive benign bone tumour, histologically characterised by a vascular stroma containing oval or spindle-shaped mononuclear neoplastic cells with a uniformly distributed multi-nucleated giant cells. (4) The multi-nucleate giant cells resemble osteoclasts and contain various enzymes and are responsible for the bone resorption in GCTB. (2) GCTB is a tumour of young adults who have achieved skeletal maturity and more than half of the cases are in their third and fourth decade as was observed in our series, with 55.1 % patients (n=16) in the third and fourth decade of their life. (2, 5) As per the published literature, 80 % of the lesions occur between 20 to 55 years of age which is comparable to our 79.3 % in 20 to 50 year age group. (1) GCTB is a rare diagnosis in skeletally immature patients with less than 3 % cases reported in patients below age of 14years. (6) A slight predilection for females has been seen in our series as in the world literature with reported male to female ratio ranging from 1:1.1 to 1:1.5. (1) The knee is the most common site accounting for 50 to 65 % of the cases. 51.6 % (n=15) of our lesions were around the knee joint. The distal femur (23 to 30 %) is the most common individual location followed by proximal tibia (20 to 25 %) and distal radius (10 to 12 %). (1) In our case, the proximal tibia was the most common site involved followed by the distal femur and distal radius. Comunoglu N et al also in their series of 120 specimens had proximal tibia as the most predominant involved site. (7) Up to 15 % of cases have been reported to involve flat bones like pelvis, scapula, ribs and calvaria. Spine, small bones of hand and feet, and patella are atypical sites for GCTB and when involved multi-centric involvement and associated Paget's disease need to be ruled out. (1, 8) We did not have any atypical site of involvement except for one case involving talus.

Symptoms of GCTB are nonspecific with pain and local swelling being the most common presentation, seen in 86 % of the patients. (9) Pain is due to mechanical insufficiency resulting from bone destruction. Local swelling may result

from the expansion of the bone or due to soft-tissue extension of the tumour mass through a cortical breach. Interference with the adjacent joint function is a presentation because of juxta-articular nature of the pathology. (2) Presentation with acute onset pain is a feature of pathological fracture that was present in 10.3 % of our cases (n=3) and as per the published literature, the incidence of pathological fracture ranges from 10 to 35 %, especially in the weight-bearing bones of the lower extremity (10, 11).

Classically the lytic lesion has a metaphyseal-epiphyseal location. Historically it was believed to arise from the epiphysis, but recent literature supports its origin from the metaphyseal side of the growth plate and as the physis closes at the maturity the lesion grows towards the epiphysis and sub-chondral bone. Cases of GCTB presenting before maturity have been reported in the literature and such lesions are always metaphyseal because the growth plate acts as a barrier to tumour expansion towards the epiphysis. (12, 13, 14) We had one case of a metaphyseal GCT where the tumour was abutting the physis scar in an adolescent female. Diaphyseal involvement suggests long-lasting disease in younger patients that has involved the diaphysis after presenting in the metaphysis. This was seen in two of our cases. GCTB has an eccentric origin but as the tumour grows it becomes centric involving the whole of the metaphysis and epiphysis. 42 to 93 % of the lesions present at the stage when they are eccentric. (3) In our case, 64 % of lesions (n=16) were eccentric at presentation. Expansile remodelling is reported in the literature to affect 47 to 60 % of the lesions. This has been seen in 65.5 % of the lesions in our study (n=19), with cortical scalloping or thinning affecting all of our cases. Cortical penetration or a breach has been demonstrated in 33 to 55% lesions at the time of presentation. (3) The cortical breach was appreciable in 51.7 % (n=15) of the lesion on plain radiographs and the same increased to 75.9 % with the use of CT images in our series. This high incidence of cortical expansion, cortical thinning and cortical breach in our study may be related to the fact that all the cases in our group were of either Campanacci grade 2 or grade 3. Radiologically GCTB shows the geographic type of bone destruction, with a clear distinction and narrow transition zone between the lesion and the normal bone. The sclerotic rim at the periphery is characteristically absent and there are reports stating that it is seen in only 1 to 2 % cases. (3) But some say a certain amount of sclerosis at the rim is not infrequent and incidence may be as high as 20 % on CT imaging. (3) In our series a definitive sclerotic rim was present in about 17.2 % lesions (n=5) on simple radiographs. A fine hair-like rim which is difficult to appreciate was seen in 44.8 % (n=13). For this reason, we have divided the transition zone in GCTB as fine hairline like sclerosis, definitive sclerotic rim, absent sclerosis but well-defined margin and absent sclerosis with wide transition zone which is suggestive of permeation and aggressive nature. Therefore, the more sclerosis, the less is the local aggressive behaviour of GCTB. Aggressive lesions with a wide transition zone constitute 10 to 20 % of the cases. (3) 24 % of our cases (n=7) were aggressive with a wide zone of transition. Scalloping effect of the lobular mass creates ridges on the endosteal surface of the cortex

which is seen as fine or coarse pseudo-trabeculations and gives the lesion honeycombed or a soap bubble appearance. (15, 16) This may be absent in more aggressive tumours where there is rapid destruction of the cortex. Pseudo-trabeculations are seen in 33 to 57 % of the lesions. (3) In our series, 62.1 % of the lesions had these pseudo-trabeculations present in part or whole of the lesion on plain radiographs.

MRI is a useful tool and gives better delineation of intra-osseous and extra-osseous limits of the lesion. Soft-tissue or extra-osseous invasion has been reported to be present in 33 to 44 % patients at the presentation. (17) 48.3 % of our cases (n=14) had some degree of soft-tissue extension on MRI images. Nothing has been mentioned in the literature about the change in the contour of the articular cartilage due to expansile nature of the lesion and due to loss of the underlying bony support. When such cartilage, with a weak underlying subchondral bone, is subjected to stress especially in the weight-bearing bones of the lower limb, the cartilage tends to deform over a course of time. Such deformed articular cartilage was seen in 34.5 % of our cases (n=10). 84 to 99 % of the lesions usually extend to within 1 cm of the sub-articular bone. (18) In our study, 89.7 % of lesions (n=26) were within 5 mm and 93 % (n=27) within 1 cm of the sub-chondral margin. The articular cartilage and underlying subchondral bone are usually resistant to tumour invasion and the articular cartilage is usually preserved till late in the disease. (2, 19) This phenomenon has made it possible to salvage the joints even in advanced stages of the disease. However, close proximity to the joint as it occurs in the distal radius may affect the ability to perform an appropriate excision and curettage which translates in higher recurrence rates. (20).

The MRI findings depicting the lesion are non-specific. (8) The consensus is that solid tumour component in the majority of the lesions is hypo to iso-intense in signal intensity with respect to the muscle in both T1 and T2 weighted images. But lesion as a whole may demonstrate heterogeneous signal intensity on T2 weighted images. (21) 48.3 % of the lesions (n=14) were of heterogeneous signal intensity on T2 images in our series. The solid component was hypo to iso-intense on T1 weighted sequence in 93.1 % of our lesions (n=27) and 72.4 % (n=21) on T2 weighted sequence. This low to intermediate signal intensity in the solid component of the lesion has been attributed to hemosiderin deposition, dense collagen matrix and high cellularity. (3, 21, 22) Long-standing cases of GCTB have a central area of necrosis, haemorrhage and cyst formation. (23) 48.3 % demonstrated cystic areas in at least some portion of the lesion on T2 sequence in our series (n=14). Areas showing fluid-fluid levels were seen in 13.8 % (n=4) of the lesions on T2 weighted images with a reported incidence of 10 to 14 % in the literature. Their presence is suggestive of secondary ABCs. (1, 24, 25) Pereira HM et al had a high incidence (53.4 %) of secondary ABC component in their series of 30 patients that was confirmed by histopathology. (9) Presence of secondary ABCs and cystic component on MRI has a clinical significance. Biopsy in GCTB should always be directed at the solid tumour component rather than cystic component, otherwise, the lesion may be misdiagnosed as a primary ABC rather than GCTB. Besides GCTB associated with secondary ABCs are more aggressive. (1, 9) Intra-tumoral hemosiderin

deposition is a feature of GCTB, attributed to phagocytosis of extravasated red blood cells. This deposition is an important factor for varied MRI picture of GCTB. Hypointensity, a feature of solid tumour component has been attributed to the presence of hemosiderin. Occasionally, these deposits are seen as nodular, whorled, zonal or diffuse hypoechoic areas in the solid tumour component. (21, 26, 27) We had such a picture of nodular hypoechoic lesions in only two (10.3 %) patients. Aoki J et al in their series of 10 patients had this phenomenon in 63 % cases. (27) However, further studies with a substantiated histopathological demonstration of such deposits are warranted.

GCTB is benign bone pathology with a spectrum of clinical-radiological presentation and classically presents as a epiphyseal-metaphyseal, eccentric, lytic lesion with pseudo-trabeculations, in a patient with closed physis growth plates. The MRI picture is variable from case to case and a surgeon should know these variations for taking a biopsy from the proper site of the lesion to prevent misdiagnosis. Association of secondary ABCs and

hemosiderin deposition is variable and needs further studies with a histopathological correlation.

#### Acknowledgements

We do not have any acknowledgements and grants or funding source for the publication of this research work.

**Conflict of Interest:** We do not have any conflict of interest in publication of this research work.

**Financial support:** We do not have financial assistance of any kind in publication of this manuscript.

Nadeem Ali, MS Orthopaedics<sup>1</sup>  
Azad Ahmad Shah, MS, DNB Orthopaedics<sup>1</sup>  
Ibreez Rakshan, MBBS<sup>1</sup>  
Altaf Ahmad Kawoosa, MS Orthopaedics<sup>1</sup>  
Mohammad Umar Mumtaz, MS Orthopaedics<sup>1</sup>  
1 Govt Medical College Srinagar, India

#### REFERENCES

- Mavrogenis AF, Igoumenou VG, Megaloikononimos PD, Panagopoulos GN, Papagelopoulos PJ, Soucacos PN. Giant cell tumor of bone revisited. *Sicot-j*. 2017;3.
- Sobti A, Agrawal P, Agarwala S, Agarwal M. Giant cell tumor of bone-an overview. *Archives of Bone and Joint Surgery*. 2016;4(1):2-9.
- Murphey MD, Nomikos GC, Flemming DJ, Gannon FH, Temple HT, Kransdorf MJ. Imaging of giant cell tumor and giant cell reparative granuloma of bone: radiologic-pathologic correlation. *Radiographics*. 2001;21(5):1283-309.
- Forsyth RG, De Boeck G, Bekaert S, De Meyer T, Taminiau AH, Uyttendaele D, et al. Telomere biology in giant cell tumour of bone. *The Journal of Pathology: A Journal of the Pathological Society of Great Britain and Ireland*. 2008;214(5):555-63.
- McGrath PJ. Giant-cell tumour of bone: an analysis of fifty-two cases. *J Bone Joint Surg Br*. 1972;54(2):216-29.
- Mendenhall WM, Zlotecki RA, Scarborough MT, Gibbs CP, Mendenhall NP. Giant cell tumor of bone. *American journal of clinical oncology*. 2006;29(1):96-9.
- Comunoglu N, Kepil N, Dervisoglu S. Histopathology of giant cell tumors of the bone: With special emphasis on fibrohistiocytic and aneurismal bone cyst like components. *Acta Orthop Traumatol Turc*. 2019;53(1):35-9.
- Chakarun CJ, Forrester DM, Gottsegen CJ, Patel DB, White EA, Matcuk Jr GR. Giant cell tumor of bone: review, mimics, and new developments in treatment. *Radiographics*. 2013;33(1):197-211.
- Pereira HM, Marchiori E, Severo A. Magnetic resonance imaging aspects of giant-cell tumours of bone. *J Med Imaging Radiat Oncol*. 2014;58(6):674-8.
- Elshenawy MA, Badran AA, Memon MA, Elshentenawy AM, Elhassan T. Outcome of treatment in giant cell tumors of bones: A single institutional retrospective review. *Annals of Oncology*. 2018;29:viii589.
- van der Heijden L, Dijkstra PS, Campanacci DA, Gibbons CM, van de Sande MA. Giant cell tumor with pathologic fracture: should we curette or resect?. *Clinical Orthopaedics and Related Research*. 2013;471(3):820-9.
- Turcotte RE. Giant cell tumor of bone. *Orthop Clin North Am*. 2006;37:35-51.
- Raskin KA, Schwab JH, Mankin HJ, Springfield DS, Hornicek FJ. Giant cell tumor of bone. *JAAOS-Journal of the American Academy of Orthopaedic Surgeons*. 2013;21(2):118-26.
- Futamura N, Urakawa H, Tsukushi S, Arai E, Kozawa E, Ishiguro N, et al. Giant cell tumor of bone arising in long bones possibly originates from the metaphyseal region. *Oncology letters*. 2016;11(4):2629-34.
- Miller TT. Bone tumors and tumor like conditions: analysis with conventional radiographs. *Radiology*. 2008;246(3):662-74.
- Manaster BJ, Doyle AJ. Giant cell tumors of bone. *Radiol Clin North Am*. 1993;31:299-323.
- Levine E, desmet AA, Neff JR. Role of radiologic imaging in management planning of giant cell tumor of bone. *Skeletal Radiol*. 1984;12:79-89.
- Murphey MD, Nomikos GC, Flemming DJ, Gannon FH, Temple HT, Kransdorf MJ. Imaging of giant cell tumor and giant cell reparative granuloma of bone: radiologic-pathologic correlation. *Radiographics*. 2001;21(5):1283-309.
- Pardiwala DN, Vyas S, Puri A, Agarwal MG. Pictorial essay: Giant cell tumor of bone. *Indian Journal of Radiology and Imaging*. 2001;11(3):119.
- Lans J, Ofazoglu K, Lee H, Harness NG, Castelein RM, Chen NC, et al. Giant Cell Tumors of the Upper Extremity: Predictors of Recurrence. *The Journal of Hand Surgery*. 2020;45(8):738-45.
- Girish G, Finlay K, Morag Y, Brandon C, Jacobson J, Jamadar D. Imaging review of skeletal tumors of the pelvis—part I: benign tumors of the pelvis. *The Scientific World Journal*. 2012;2012.
- Kwon JW, Chung HW, Cho EY, Hong SH, Choi SH, Yoon YC, et al. MRI findings of giant cell tumors of the spine. *American Journal of Roentgenology*. 2007 Jul;189(1):246-50.
- Haque AU, Moatasim A. Giant cell tumor of bone: a neoplasm or a reactive condition? *Int J Clin Exp Pathol*. 2008;1(6):489-501.

24. Kaplan PA, Murphey M, Greenway G, Resnick D, Sartoris DJ, Harms S. Fluid-fluid levels in giant cell tumors of bone: report of two cases. *Journal of Computed Tomography*. 1987;11(2):151-5.
25. Anchan C. Giant cell tumor of bone with secondary aneurysmal bone cyst. *Int J Shoulder Surg*. 2008;2(3):68.
26. Aoki J, Moriya K, Yamashita K, Fujioka F, Ishii K, Karakida O, et al. Giant cell tumors of bone containing large amounts of hemosiderin: MR-pathologic correlation. *Journal of computer assisted tomography*. 1991;15(6):1024-7.
27. Aoki J, Tanikawa H, Ishii K, Seo GS, Karakida O, Sone S, et al. MR findings indicative of hemosiderin in giant-cell tumor of bone: frequency, cause, and diagnostic significance. *AJR. American journal of roentgenology*. 1996;166(1):145-8.